Accurate nuclear symmetry energy at finite temperature within a Brueckner-Hartree-Fock approach

Fan Li (李凡), Jia-Jing Lu (陆家靖), Zeng-Hua Li (李增花),* and Chong-Yang Chen (陈重阳)
Institute of Modern Physics, Key Laboratory of Nuclear Physics and Ion-Beam Application (MOE), Fudan University, Shanghai 200433, People's Republic of China

G. F. Burgio and H.-J. Schulze
INFN Sezione di Catania, Dipartimento di Fisica, Universitá di Catania, Via Santa Sofia 64, 95123 Catania, Italy

(Received 21 April 2020; revised 5 December 2020; accepted 19 January 2021; published 5 February 2021)

We compute the free energy of asymmetric nuclear matter in a Brueckner-Hartree-Fock approach at finite temperature, paying particular attention to the dependence on isospin asymmetry. The first- and second-order symmetry energies are determined as functions of density and temperature and useful parametrizations are provided. We find small deviations from the quadratic isospin-asymmetry dependence and very small corresponding effects on (proto)neutron star structure.

DOI: 10.1103/PhysRevC.103.024307

I. INTRODUCTION

The nuclear symmetry energy, i.e., the energy difference between removing a neutron or a proton from nuclear matter [1], is an important topic of experimental and theoretical nuclear (astro)physics, as it affects a large number of phenomena in nuclear structure physics [2], heavy-ion collisions [3–5], and astrophysics like neutron star (NS) structure [6–9] or recently NS mergers [10–14]. In heavy-ion collisions at intermediate and high energy induced by radioactive beams, rare isotopes with extreme proton-to-neutron ratios are created, and their existence and structure such as the neutron skin thickness are intimately related to the nuclear symmetry energy. In the interior of NSs the composition and pressure are dominantly determined by the symmetry energy and its slope parameters. Consequently, the overall structure of NSs including the radius, momentum of inertia, and crust-core transition density depends sensitively on the symmetry energy. Moreover, in binary NS mergers the symmetry energy also plays an essential role for understanding the dynamical properties of rotating neutron stars and the associated gravitational-wave signatures.

In all the above scenarios, the nuclear system might be at non-negligible finite temperature of the order of several tens of MeV. This requires to consider the free energy as a fundamental thermodynamical quantity. Therefore in recent years some phenomenological methods, such as a momentum-dependent effective interaction [15] and the nuclear energy-density functional theory [16], were applied to the study of the behavior of the free energy of nuclear matter as a function of the baryon density and temperature. More recently, microscopic calculations based on the self-consistent Green's function method with nuclear forces derived from chiral effective field theory were performed [17]. Further microscopic calculations have also been carried out in the framework of the correlated basis function theory [18] and applied to the simulations of the evolution of a protoneutron star [19]. Moreover, we have computed the free energy up to large nucleon densities $\rho \lesssim 0.8\ \mathrm{fm}^{-3}$ and temperatures $T \lesssim 50$ MeV within the theoretical Brueckner-Hartree-Fock (BHF) method, and provided convenient parametrizations for practical use [20].

Under these circumstances, the nuclear free (symmetry) energy depends on the partial densities ρ_n and ρ_p, and temperature T. An important feature is the dependence on isospin asymmetry $\beta \equiv (\rho_n - \rho_p)/(\rho_n + \rho_p)$ for fixed nucleon density $\rho = \rho_n + \rho_p$, and for cold matter it has been demonstrated that a quadratic dependence $\sim\beta^2$ is rather accurate [21–26]. However, at finite temperature this approximation becomes less reliable [27–30] and one should seek to go beyond this lowest-order parametrization. This is the focus of the present article, where we study in detail the dependence of the finite-temperature free energy on isospin asymmetry and provide parametrizations that go beyond the quadratic law. We will also give a simple application to NS structure in order to estimate the magnitude of the effect in practical applications.

We consider in this work two microscopic equations of state (EOSs) that have been derived within the BHF formalism [2,31–34] based on realistic two-nucleon (NN) and compatible three-nucleon forces (TBFs) [35–39], namely, those employing the Argonne V_{18} [40] or the Bonn B [41,42] NN potentials, respectively. They all feature reasonable properties at (sub)nuclear densities in agreement with nuclear-structure phenomenology [39,43–45], and are also fully compatible with recent constraints obtained from the analysis of the GW170817 NS merger event [46–48], as well as from NS cooling [49–51].

*zhli09@fudan.edu.cn

Recently first numerical simulations of NS merger events were performed with the BHF V18 finite-temperature EOS [52] and it was found that during the postmerger phase maximum temperatures $T \approx 70$ MeV can be reached in small domains of spacetime with this EOS, whereas the average temperature during the first milliseconds of life is about 20 MeV. In simulations of protoneutron star evolution [19,53], the maximum temperatures are somewhat lower, $T \lesssim 50$ MeV. This sets the scale for typical temperatures to be addressed in the theoretical approach.

Our paper is organized as follows. In Sec. II we briefly review the computation of the free energy in the finite-temperature BHF approach and give some details of the fitting procedure. In Sec. III we present the numerical results for the free energy with particular regard to the dependence on isospin asymmetry, and some model calculations of hot NS structure. Conclusions are drawn in Sec. IV.

II. FORMALISM

The calculations for hot asymmetric nuclear matter are based on the Brueckner-Bethe-Goldstone (BBG) theory [21,23,31–34] and its extension to finite temperature [27,54–59]. Here we simply give a brief review for completeness.

We employ the BHF approach for asymmetric nuclear matter at finite temperature to calculate the free energy density in the "frozen-correlations" approximation,

$$f = \rho\frac{F}{A} = \sum_{i=n,p}\left[2\sum_k n_i(k)\left(\frac{k^2}{2m_i}+\frac{1}{2}U_i(k)\right) - T s_i\right], \quad (1)$$

where

$$s_i = -2\sum_k\{n_i(k)\ln n_i(k) + [1-n_i(k)]\ln[1-n_i(k)]\} \quad (2)$$

is the entropy density for the component i treated as a free Fermi gas with spectrum $e_i(k)$. At finite temperature,

$$n_i(k) = \left[\exp\left(\frac{e_i(k)-\tilde{\mu}_i}{T}\right)+1\right]^{-1} \quad (3)$$

is a Fermi distribution, where the auxiliary chemical potentials $\tilde{\mu}_{n,p}$ are fixed by the condition $\rho_i = 2\sum_k n_i(k)$. The single-particle energy

$$e_1 = \frac{k_1^2}{2m_1} + U_1, \quad (4)$$

$$U_1(\rho, x_p) = \sum_2 n_2\langle 12|K(\rho, x_p; e_1+e_2)|12\rangle_a, \quad (5)$$

is obtained from the interaction matrix K, which satisfies the Bethe-Goldstone integral equation

$$K(\rho, x_p; E) = V + V\,\mathrm{Re}\sum_{1,2}\frac{|12\rangle(1-n_1)(1-n_2)\langle 12|}{E-e_1-e_2+i0}K(\rho, x_p; E). \quad (6)$$

Here E is the starting energy and $x_p = \rho_p/\rho$ is the proton fraction. The multi-indices 1,2 denote in general momentum, isospin, and spin. At given baryon density and proton fraction, Eqs. (3)–(6) are solved self-consistently until the K matrix reaches convergence. Then the free energy density and entropy density are calculated according to Eqs. (1) and (2).

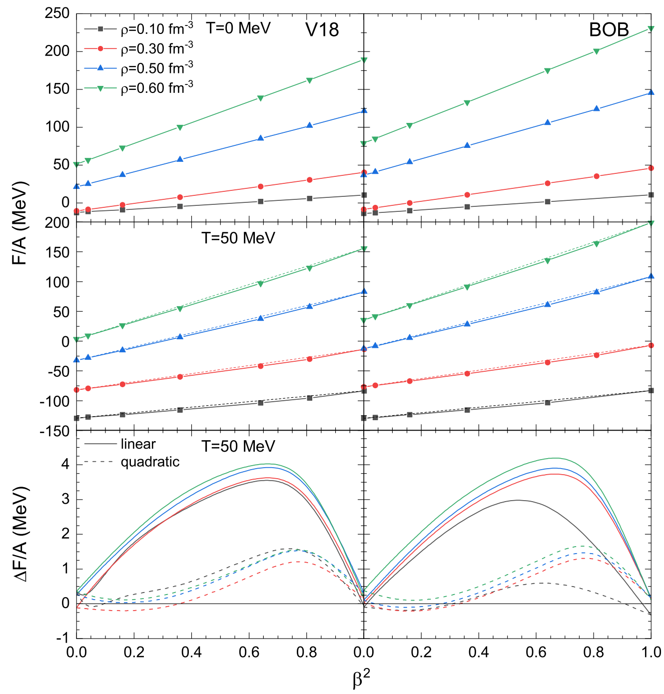

FIG. 1. Free energy per nucleon as a function of asymmetry for different densities at $T = 0$ (top panels), 50 MeV (middle panels) for the V18 (left panels) or BOB (right panels) EOS. Dashed straight lines in those panels show the parabolic approximation, Eq. (11). The bottom panels show the deviation between numerical results and the linear [Eq. (11), solid curves] or quadratic [Eq. (12), dashed curves] β^2 fits.

The frozen-correlations approximation consists in using in the latter step the single-particle energy in Eq. (4) computed at zero temperature instead of finite temperature. It has been shown that at not too high temperature ($T \lesssim 30$ MeV) this produces a negligible effect on thermodynamic properties of nuclear matter [34,58–61]. Even in the most extreme situation of low density $\rho \approx 0.1\ \mathrm{fm}^{-3}$ (the BHF approach is not used for inhomogeneous clustered nuclear matter below that value) and high temperature $T = 50$ MeV, the accuracy of that approximation is about 5 MeV (5%) for F/A, but much better for higher density and lower temperature [61]. In comparison, the quadratic isospin law analyzed later is violated by a few MeV ($\lesssim 4$ MeV, see Fig. 1) throughout most of the parameter space.

Two choices for the realistic NN interaction V are adopted in the present calculations [39]: the Argonne V_{18} (V18) [40] and the Bonn B (BOB) [41,42] potential. They are supplemented with microscopic TBF employing the same meson-exchange parameters as the two-body potentials. The TBF is reduced to an effective two-body force and added to the bare potential in the BHF calculation (see Refs. [37–39,62] for details).

The knowledge of the free energy allows to derive all necessary thermodynamical quantities in a consistent way;

namely, one defines the "true" chemical potentials μ_i, pressure p, and internal energy density ϵ as

$$\mu_i = \frac{\partial f}{\partial \rho_i}\,, \tag{7}$$

$$p = \rho^2 \frac{\partial (f/\rho)}{\partial \rho} = \sum_i \mu_i \rho_i - f\,, \tag{8}$$

$$\epsilon = f + Ts\,, \quad s = -\frac{\partial f}{\partial T}. \tag{9}$$

For the case of asymmetric nuclear matter, one might expand the free energy for fixed total density and temperature in terms of the asymmetry parameter $\delta = \beta^2 = (1-2x_p)^2$,

$$f(\delta) \approx f(0) + \delta f_{\mathrm{sym},2} + \delta^2 f_{\mathrm{sym},4}. \tag{10}$$

Limiting to the second term, one obtains the symmetry energy as the difference between pure neutron matter (PNM) and symmetric nuclear matter (SNM),

$$f_{\mathrm{sym},2} = f(1) - f(0), \tag{11a}$$

$$f_{\mathrm{sym},4} = 0, \tag{11b}$$

which is usually a good approximation at zero temperature [21,23,61], and also used at finite temperature [19,27]. It has, however, been pointed out [28–30,63–70] that at least the kinetic part of the free energy density [first term in Eq. (1)] violates the parabolic law, in particular at high temperature. We therefore extend the expansion to second order and compute $f_{\mathrm{sym},4}$ in the following way: Inverting the system of equations for $f(0)$, $f(\alpha)$, and $f(1)$, where α is an arbitrarily chosen value (we use $\alpha = 0.6^2$, which corresponds to a typical $x_p = 0.2$ in NS matter), one obtains

$$f_{\mathrm{sym},2} = \frac{\alpha^2[f(1)-f(0)] - [f(\alpha)-f(0)]}{\alpha^2 - \alpha}, \tag{12a}$$

$$f_{\mathrm{sym},4} = \frac{\alpha[f(1)-f(0)] - [f(\alpha)-f(0)]}{\alpha - \alpha^2}, \tag{12b}$$

in which $f(0)$, $f(\alpha)$, and $f(1)$ depend on total density and temperature. Following Ref. [20], we provide analytical fits for these dependencies of the numerical results in the required ranges of density ($0.05 \lesssim \rho \lesssim 1\ \mathrm{fm}^{-3}$) and temperature ($5 \leqslant T \leqslant 50$ MeV) in the following functional form for the free energy per nucleon:

$$\frac{F}{A}(\rho,T) = a\rho + b\rho^c + d + \tilde{a}t^2\rho + \tilde{b}t^2\ln(\rho) + (\tilde{c}t^2 + \tilde{d}t^{\tilde{e}})/\rho, \tag{13}$$

where $t = T/(100\ \mathrm{MeV})$ and F/A and ρ are given in MeV and fm^{-3}, respectively. The parameters of the fits are listed in Table I for SNM, asymmetric nuclear matter with $x_p = 0.2$ (ANM), and PNM, for the different EOSs we are using. The rms deviations of fits and data are better than 0.3 MeV for all EOSs and also given in the table. We stress that the main purpose of the chosen functional form is a good fit of the numerical data in an economical way, valid only in the stated ranges of density and temperature. Thus theoretical interpretations should be taken with care, also in view of strong compensations between the individual terms. Different functional forms of such fits have been proposed in the literature, taking into account only the interaction part of the free energy [19], and we have verified that the accuracies of the fits for SNM, ANM, and PNM, as reported in Table I, are much better than the effect of using different parametrizations for the isospin dependence that we are investigating here.

TABLE I. Parameters of the fit for the free energy per nucleon, F/A, Eq. (13), for symmetric nuclear matter (SNM), asymmetric ($\beta = 0.6$) nuclear matter (ANM), and pure neutron matter (PNM) with the V18 and BOB EOSs. The accuracies $\langle \Delta F/A \rangle_{\mathrm{rms}}$ (in MeV) are also listed.

		a	b	c	d	$\tilde{a}$	$\tilde{b}$	$\tilde{c}$	$\tilde{d}$	$\tilde{e}$	$\langle \Delta F/A \rangle$
V18	SNM	−54	363	2.68	−8	−149	211	−58	81	2.40	0.21
	ANM	−23	473	2.72	−3	−140	200	−61	82	2.36	0.17
	PNM	38	668	2.78	6	−91	153	−26	38	2.64	0.18
BOB	SNM	−60	495	2.69	−9	−124	203	−60	80	2.38	0.29
	ANM	−21	624	2.78	−4	−119	193	−59	78	2.36	0.22
	PNM	52	860	2.89	4	−82	149	−25	36	2.67	0.20

III. RESULTS

A. Free energy per nucleon

Figure 1 shows the free energy per nucleon as a function of the asymmetry parameter $\delta = \beta^2$ for different densities and at temperatures $T = 0$ (upper row) and $T = 50$ MeV (middle row), for both EOSs. The linear approximation [Eqs. (10) and (11)] is indicated by dashed straight lines in those panels, and the deviations from the linear [Eq. (11)] or quadratic [Eq. (12)] laws at $T = 50$ MeV are indicated in the lower row. One observes that in general even the linear law provides a very good fit, even at low density and high temperature, where the deviations might reach a few percent. With the quadratic law, the deviations remain below 2 MeV over the whole parameter space $[\rho, T, \beta]$. In this case the overall variances are 0.47 and 0.54 MeV for the V18 and BOB EOSs, respectively.

In order to compare the magnitude of violation of the linear or quadratic β^2 laws with those of other frequently used finite-temperature nuclear EOSs, we performed the previous analysis also for the SFHo [71] and the HShen [72,73] EOSs and report the values of the variance $\langle \Delta F/A \rangle_{\mathrm{rms}}$ for both the linear and quadratic law in Table II. We observe that in all cases the quadratic law is an important improvement by at least a factor of 3, but also the linear law is a very reasonable approximation. In the table we report also the results obtained with two other values of $\alpha = 0.4^2$ and 0.8^2 ($x_p = 0.3$ and 0.1)

TABLE II. Quality $\langle \Delta F/A \rangle_{\mathrm{rms}}$ (in MeV) of the linear or quadratic β^2 laws for the free energy per nucleon, F/A, obtained with different EOSs and different choices of α in Eq. (12).

EOS	V18	BOB	SFHo	Shen
Linear	1.51	1.77	1.12	1.53
Quadratic ($\alpha = 0.4^2$)	0.57	0.67	0.35	0.50
Quadratic ($\alpha = 0.6^2$)	0.47	0.54	0.23	0.39
Quadratic ($\alpha = 0.8^2$)	0.42	0.48	0.30	0.34

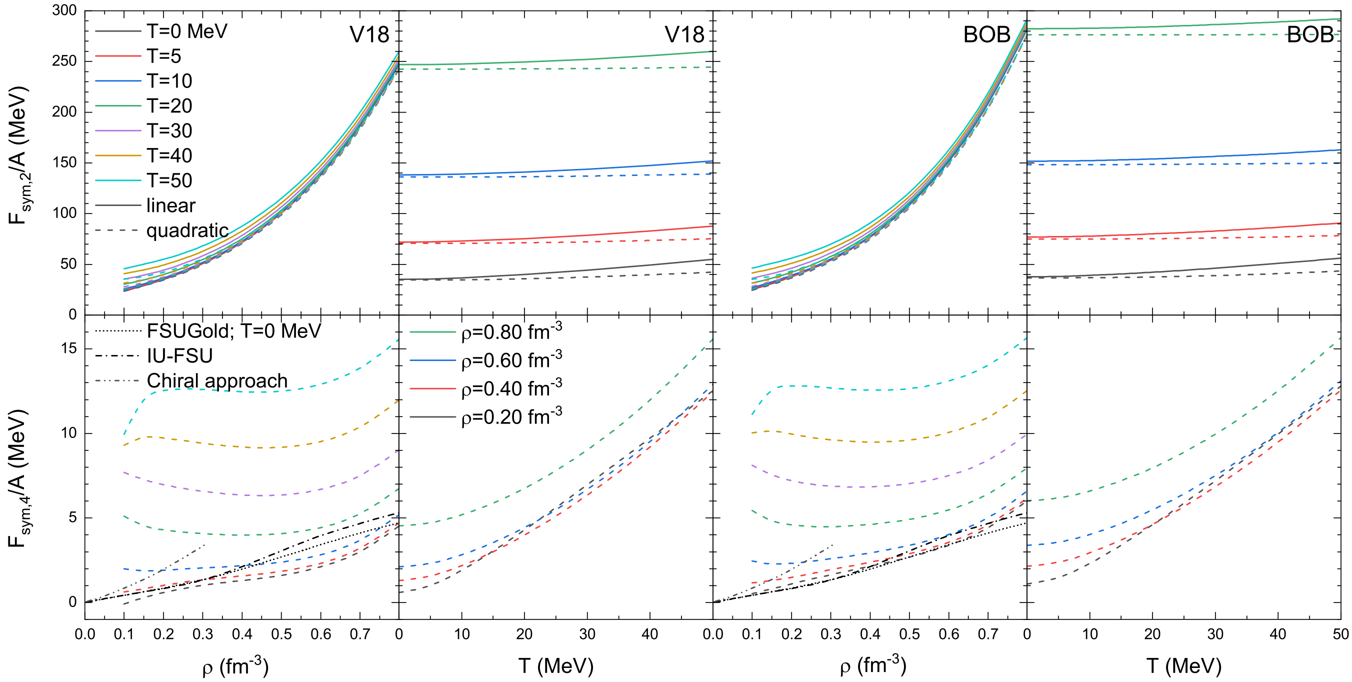

FIG. 2. Free symmetry energies per nucleon, $F_{\mathrm{sym},2}/A$ (upper row; in linear [Eq. (11), solid curves] or quadratic [Eq. (12), dashed curves] approximation) and $F_{\mathrm{sym},4}/A$ (lower row) as functions of nucleon density or temperature for fixed temperatures and densities, respectively. For comparison, the $T = 0$ FSUGold and IU-FSU results of Ref. [74] and those of Ref. [75] are plotted in the lower row.

in Eq. (12) in order to demonstrate the invariance of the main conclusions with respect to this choice.

Figure 2 shows the derived free symmetry energies per nucleon, $F_{\mathrm{sym},2}/A$ [Eqs. (11a) and (12a)] and $F_{\mathrm{sym},4}/A$ [Eq. (12b)], as functions of density and temperature. One notes that the dependence on density is more pronounced for $F_{\mathrm{sym},2}/A$ than for $F_{\mathrm{sym},4}/A$, while the opposite is the case for the temperature dependence. The $F_{\mathrm{sym},2}/A$ results in quadratic approximation (dashed curves in upper row) are somewhat smaller than in linear approximation (solid curves) in order to compensate for the finite $F_{\mathrm{sym},4}/A$, in particular at finite temperature. For comparison, the $T = 0$ results for $F_{\mathrm{sym},4}/A$ obtained by Relativistic Mean Field (RMF) theory with FSU interactions [74] and those of the schematic chiral model [75] are shown as dotted, dash-dotted, and dash-dot-dotted curves in the lower row. The former are comparable with our BHF results, especially the BOB model.

B. Results at normal density

The density dependence of the symmetry energies can be expanded around normal density $\rho_0 = 0.17\ \mathrm{fm}^{-3}$ in terms of normal values J_2 and J_4 and slope parameters L_2 and L_4:

$$F_{\mathrm{sym},2}/A(\rho, T) \approx J_2(T) + L_2(T)x, \tag{14}$$

$$F_{\mathrm{sym},4}/A(\rho, T) \approx J_4(T) + L_4(T)x, \tag{15}$$

where $x \equiv (\rho - \rho_0)/3\rho_0$ and $J_i(T) = J_{\mathrm{sym,i}}(\rho_0, T)$, $L_i(T) = 3\partial J_{\mathrm{sym,i}}(\rho_0, T)/\partial\rho$. These quantities are shown in Fig. 3. The $T = 0$ values are $J_2(0) = 31.0$ (32.7) MeV and $L_2(0) = 58.5$ (64.2) MeV for V18 (BOB), which should be confronted with recent constraints $J_2 = 31.7 \pm 2.7$ MeV and $L_2 = 58.7 \pm 28.1$ MeV [7,76]. In the same figure we report also the results for the SFHo and Shen EOSs according to our analysis (see also Table II). Reasonable values are obtained in the first case, but too large ones in the latter.

The second-order symmetry energy $J_4(0)$ is theoretically more controversial than the first-order one, $J_2(0)$. Our results are $J_4(0) = 0.41$, 0.93, 1.17, and 1.17 MeV for the V18, BOB, SFHo, and Shen EOSs, respectively. Within energy-density functionals with mean-field approximation,

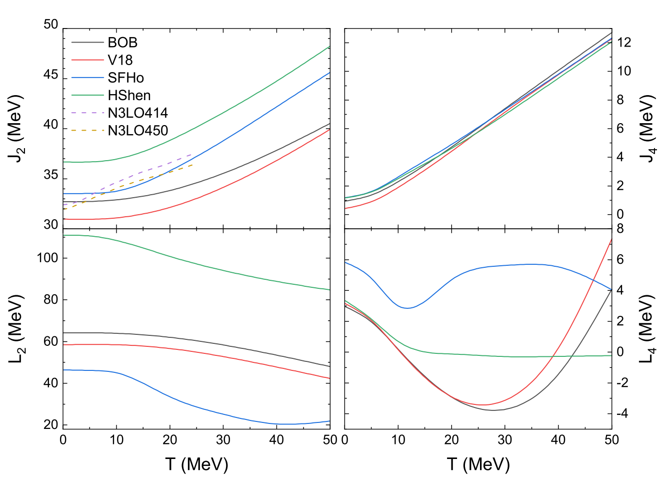

FIG. 3. Symmetry energies J_2 and J_4 (upper panels) and slope parameters L_2 and L_4 (lower panels) at empirical saturation density $\rho_0 = 0.17\ \mathrm{fm}^{-3}$ as a function of temperature for different EOSs. The N3LO414 and N3LO450 results of Ref. [30] are plotted as dashed curves.

for example, Skyrme-Hartree-Fock and Gogny-Hartree-Fock models, the values of J_4 reported in the literature are around 1.0 MeV [66], and around 0.66 MeV within RMF models [74], while values extracted from quantum molecular dynamics models could be larger depending on the specific interaction [64]. A recent analysis in second-order chiral perturbation theory [75] obtains $J_4 \approx 1.5$ MeV and proposes to modify the expansion Eq. (10) by a $\delta^2 \ln \delta$ term. (See also Ref. [77], where even negative J_4 values were extracted.)

From the viewpoint of finite nuclei, J_4 can be related to the second-order symmetry energy $a_{\mathrm{sym},4}(A)$ in a semiempirical mass formula, which can be inferred from the double differences of experimental binding energies by analyzing a large number of measured nuclei [78,79]. In this case, the estimates are $J_4 = 20.0 \pm 4.6$ MeV [78] and two possible $J_4 = 8.5 \pm 0.5$ MeV or $J_4 = 3.3 \pm 0.5$ MeV [79], which are significantly different and much larger than those deduced from nuclear matter. This points to a great model dependence and to the importance of finite-size effects in nuclei.

Regarding the temperature dependence, from Fig. 3 one can see that $J_2(T)$ and $J_4(T)$ are increasing monotonically with temperature for all models, whereas $L_2(T)$ decreases and $L_4(T)$ exhibits nonmonotonic behavior. It is remarkable that the $J_4(T)$ results are nearly universal for all EOSs. Note that in our approach the temperature dependence of all these quantities is constrained to be a linear combination of T^2 and $T^{\tilde{e}}$ terms according to Eq. (13). We compare our results with the ones of the chiral effective field theory calculation [30]. Considering also the cutoff dependence of the chiral potentials, we observe that both results are in quantitative agreement in particular in the low-temperature region, but the latter predicts a more linear temperature dependence. (At low temperature such behavior is excluded by the condition of vanishing entropy in the $T \to 0$ limit.) The temperature dependence of the free symmetry energy is also discussed in Refs. [80,81], where an isospin- and momentum-dependent interaction constrained by heavy-ion collisions and the Skyrme SLy4 parameters have been employed, respectively. Those investigations show very similar behavior and numerical magnitudes as the present calculations of the free symmetry energy.

C. Hot neutron stars

To assess the relevance of the previous results for practical applications, we perform some model calculations of NS structure employing the different approximations for the symmetry energy. Figure 4 shows the proton fractions of β-stable and charge-neutral nuclear matter in the upper panel and the mass-radius relations of NSs in the lower panel at the temperatures $T = 0$ and $T = 50$ MeV (For this plot, a cold crust is attached to the isothermal NS interior at $\rho = 0.08$ fm^{-3} for simplicity.) Results using the linear [Eq. (11), thin curves] or the quadratic [Eq. (12), thick curves] δ laws are compared with both BOB and V18 interactions. One can see that the inclusion of $F_{\mathrm{sym},4}$ in the latter case causes a slight decrease of the proton fraction in particular at high temperature, corresponding to a slight reduction of F/A as seen in Fig. 1. The effect on the mass-radius relations is nearly invisible, even at large finite temperature, which means that the linear law in Eq. (11) is already a very good approximation for the determination of the stellar structure.

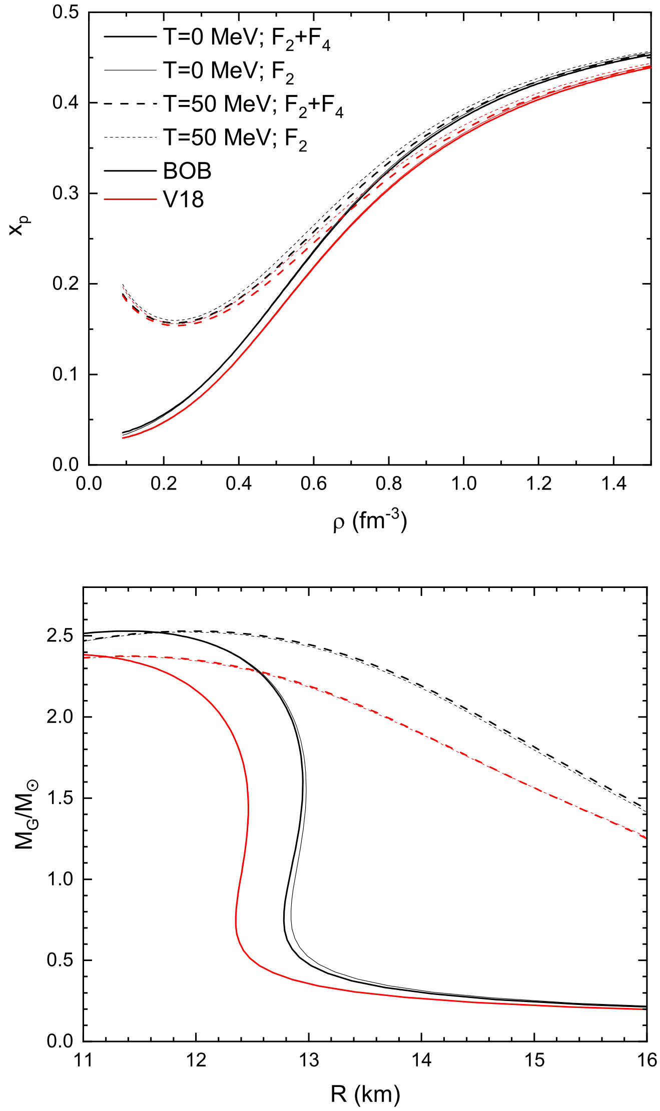

FIG. 4. Proton fraction of β-stable matter (upper plot) and NS mass-radius relation (lower plot) at $T = 0$ (solid curves) and 50 MeV (dashed curves), employing linear (thin curves) or quadratic (thick curves) β^2 fits, Eq. (11) or (12).

For the interested reader we note that a peculiarity of the finite-temperature BHF approach is the prediction of rather temperature-independent (or slightly decreasing) maximum NS masses. This is due to a strong compensation between the nucleonic and leptonic contributions to the thermal pressure, which was carefully analyzed in Refs. [20,52].

IV. SUMMARY

We studied the isospin-asymmetry dependence of the free energy of nuclear matter at zero and finite temperature within the framework of the Brueckner-Hartree-Fock approach at finite temperature with different potentials and compatible nuclear three-body forces. We compared our results with phenomenological models, i.e., SFHo and Shen EOSs, which are widely used in numerical simulations of astrophysical processes.

We determined the first- and second-order terms in an expansion with respect to isospin asymmetry and provided convenient parametrizations for practical applications. We did not find anomalously large second-order terms, and a model study of neutron star structure at finite temperature demonstrated that the often used parabolic law is an excellent approximation even at high temperature and the second-order modifications are very small.

Our results will be used in simulations of protoneutron stars and neutron star mergers, where accounting for finite temperature is an essential requirement. We plan to refine our calculations by going beyond the frozen-correlations approximation, which is less accurate at large values of temperature, especially in the low-density regime, where thermal effects play a major role. In the high-density range, which is more important for neutron star structure and their maximum mass, we do not expect important changes. This will be subject of investigation in a future paper.

ACKNOWLEDGMENTS

This work is sponsored by the National Natural Science Foundation of China under Grants No. 11475045 and No. 11975077 and the China Scholarship Council, Grant No. 201806100066. We further acknowledge partial support from "PHAROS," COST Action CA16214.

[1] M. Baldo and G. F. Burgio, Prog. Part. Nucl. Phys. **91**, 203 (2016).
[2] M. Baldo and G. F. Burgio, Rep. Prog. Phys. **75**, 026301 (2012).
[3] P. Danielewicz, R. Lacey, and W. G. Lynch, Science **298**, 1592 (2002).
[4] B.-A. Li, L.-W. Chen, and C. M. Ko, Phys. Rep. **464**, 113 (2008).
[5] M. B. Tsang *et al.*, Phys. Rev. C **86**, 015803 (2012).
[6] A. Steiner, M. Prakash, J. Lattimer, and P. Ellis, Phys. Rep. **411**, 325 (2005).
[7] B.-A. Li, P. G. Krastev, D.-H. Wen, and N.-B. Zhang, Eur. Phys. J. A **55**, 117 (2019).
[8] C. Y. Tsang, M. B. Tsang, P. Danielewicz, W. G. Lynch, and F. J. Fattoyev, arXiv:1901.07673.
[9] J. M. Lattimer and A. W. Steiner, Eur. Phys. J. A **50**, 40 (2014).
[10] B. P. Abbott *et al.* (LIGO Scientific Collaboration and Virgo Collaboration), Phys. Rev. Lett. **119**, 161101 (2017).
[11] B. P. Abbott *et al.* (LIGO Scientific Collaboration and Virgo Collaboration), Phys. Rev. Lett. **121**, 161101 (2018).
[12] B. P. Abbott *et al.* (LIGO Scientific Collaboration and Virgo Collaboration), Phys. Rev. X **9**, 011001 (2019).
[13] L. Baiotti and L. Rezzolla, Rep. Prog. Phys. **80**, 096901 (2017).
[14] L. Baiotti, Prog. Part. Nucl. Phys. **109**, 103714 (2019).
[15] C. C. Moustakidis and C. P. Panos, Phys. Rev. C **79**, 045806 (2009).
[16] A. F. Fantina, N. Chamel, J. M. Pearson, and S. Goriely, J. Phys. Conf. Ser. **342**, 012003 (2012).
[17] A. Carbone and A. Schwenk, Phys. Rev. C **100**, 025805 (2019).
[18] O. Benhar and A. Lovato, Phys. Rev. C **96**, 054301 (2017).
[19] G. Camelio, A. Lovato, L. Gualtieri, O. Benhar, J. A. Pons, and V. Ferrari, Phys. Rev. D **96**, 043015 (2017).
[20] J.-J. Lu, Z.-H. Li, G. F. Burgio, A. Figura, and H.-J. Schulze, Phys. Rev. C **100**, 054335 (2019).
[21] I. Bombaci and U. Lombardo, Phys. Rev. C **44**, 1892 (1991).
[22] C.-H. Lee, T. T. S. Kuo, G. Q. Li, and G. E. Brown, Phys. Rev. C **57**, 3488 (1998).
[23] W. Zuo, I. Bombaci, and U. Lombardo, Phys. Rev. C **60**, 024605 (1999).
[24] T. Frick, H. Müther, A. Rios, A. Polls, and A. Ramos, Phys. Rev. C **71**, 014313 (2005).
[25] I. Vidaña, C. Providência, A. Polls, and A. Rios, Phys. Rev. C **80**, 045806 (2009).
[26] C. Drischler, V. Somà, and A. Schwenk, Phys. Rev. C **89**, 025806 (2014).
[27] W. Zuo, Z. H. Li, A. Li, and G. C. Lu, Phys. Rev. C **69**, 064001 (2004).
[28] H. Togashi and M. Takano, Nucl. Phys. A **902**, 53 (2013).
[29] H. Togashi, K. Nakazato, Y. Takehara, S. Yamamuro, H. Suzuki, and M. Takano, Nucl. Phys. A **961**, 78 (2017).
[30] C. Wellenhofer, J. W. Holt, and N. Kaiser, Phys. Rev. C **92**, 015801 (2015).
[31] J. Goldstone, Proc. R. Soc. London Ser. A **239**, 267 (1957).
[32] J. P. Jeukenne, A. Lejeune, and C. Mahaux, Phys. Rep. **25**, 83 (1976).
[33] B. D. Day, Nucl. Phys. A **328**, 1 (1979).
[34] M. Baldo, in *Nuclear Methods and the Nuclear Equation of State*, International Review of Nuclear Physics Vol. 8 (World Scientific, Singapore, 1999).
[35] M. Baldo, I. Bombaci, and G. F. Burgio, Astron. Astrophys. **328**, 274 (1997).
[36] X. R. Zhou, G. F. Burgio, U. Lombardo, H.-J. Schulze, and W. Zuo, Phys. Rev. C **69**, 018801 (2004).
[37] W. Zuo, A. Lejeune, U. Lombardo, and J. F. Mathiot, Nucl. Phys. A **706**, 418 (2002).
[38] Z. H. Li, U. Lombardo, H.-J. Schulze, and W. Zuo, Phys. Rev. C **77**, 034316 (2008).
[39] Z. H. Li and H.-J. Schulze, Phys. Rev. C **78**, 028801 (2008).
[40] R. B. Wiringa, V. G. J. Stoks, and R. Schiavilla, Phys. Rev. C **51**, 38 (1995).
[41] R. Machleidt, K. Holinde, and C. Elster, Phys. Rep. **149**, 1 (1987).
[42] R. Machleidt, in *Advances in Nuclear Physics*, edited by J. W. Negele and E. Vogt (Springer, Boston, 1989), pp. 189–376.
[43] Z.-H. Li, D.-P. Zhang, H.-J. Schulze, and W. Zuo, Chin. Phys. Lett. **29**, 012101 (2012).
[44] Q.-Y. Bu, Z.-H. Li, and H.-J. Schulze, Chin. Phys. Lett. **33**, 032101 (2016).
[45] G. Taranto, M. Baldo, and G. F. Burgio, Phys. Rev. C **87**, 045803 (2013).
[46] G. F. Burgio, A. Drago, G. Pagliara, H.-J. Schulze, and J.-B. Wei, Astrophys. J. **860**, 139 (2018).
[47] J.-B. Wei, A. Figura, G. F. Burgio, H. Chen, and H.-J. Schulze, J. Phys. G **46**, 034001 (2019).

[48] J.-B. Wei, J.-J. Lu, G. F. Burgio, Z.-H. Li, and H.-J. Schulze, Eur. Phys. J. A **56**, 63 (2020).
[49] M. Fortin, G. Taranto, G. F. Burgio, P. Haensel, H.-J. Schulze, and J. L. Zdunik, Mon. Not. R. Astron. Soc. **475**, 5010 (2018).
[50] J.-B. Wei, G. F. Burgio, and H.-J. Schulze, Mon. Not. R. Astron. Soc. **484**, 5162 (2019).
[51] J.-B. Wei, F. Burgio, and H.-J. Schulze, Universe **6**, 115 (2020).
[52] A. Figura, J.-J. Lu, G. F. Burgio, Z.-H. Li, and H.-J. Schulze, Phys. Rev. D **102**, 043006 (2020).
[53] G. F. Burgio, V. Ferrari, L. Gualtieri, and H.-J. Schulze, Phys. Rev. D **84**, 044017 (2011).
[54] C. Bloch and C. De Dominicis, Nucl. Phys. A **7**, 459 (1958).
[55] C. Bloch and C. De Dominicis, Nucl. Phys. A **10**, 181 (1959).
[56] C. Bloch and C. De Dominicis, Nucl. Phys. A **10**, 509 (1959).
[57] I. Bombaci, T. T. S. Kuo, and U. Lombardo, Phys. Rep. **242**, 165 (1994).
[58] A. Lejeune, P. Grange, M. Martzolff, and J. Cugnon, Nucl. Phys. A **453**, 189 (1986).
[59] M. Baldo and L. S. Ferreira, Phys. Rev. C **59**, 682 (1999).
[60] O. E. Nicotra, M. Baldo, G. F. Burgio, and H.-J. Schulze, Astron. Astrophys. **451**, 213 (2006).
[61] G. F. Burgio and H.-J. Schulze, Astron. Astrophys. **518**, A17 (2010).
[62] P. Grangé, A. Lejeune, M. Martzolff, and J.-F. Mathiot, Phys. Rev. C **40**, 1040 (1989).
[63] N. H. Tan, D. T. Loan, D. T. Khoa, and J. Margueron, Phys. Rev. C **93**, 035806 (2016).
[64] R. Nandi and S. Schramm, Phys. Rev. C **94**, 025806 (2016).
[65] J. Margueron and F. Gulminelli, Phys. Rev. C **99**, 025806 (2019).
[66] J. Pu, Z. Zhang, and L.-W. Chen, Phys. Rev. C **96**, 054311 (2017).
[67] N. Zabari, S. Kubis, and W. Wójcik, Phys. Rev. C **100**, 015808 (2019).
[68] B.-A. Li, B.-J. Cai, L.-W. Chen, and J. Xu, Prog. Part. Nucl. Phys. **99**, 29 (2018).
[69] Z. W. Liu, Z. Qian, R. Y. Xing, J. R. Niu, and B. Y. Sun, Phys. Rev. C **97**, 025801 (2018).
[70] N. Wan, C. Xu, Z. Ren, and J. Liu, Phys. Rev. C **97**, 051302(R) (2018).
[71] A. W. Steiner, M. Hempel, and T. Fischer, Astrophys. J. **774**, 17 (2013).
[72] H. Shen, H. Toki, K. Oyamatsu, and K. Sumiyoshi, Prog. Theor. Phys. **100**, 1013 (1998).
[73] H. Shen, H. Toki, K. Oyamatsu, and K. Sumiyoshi, Astrophys. J. Suppl. Ser. **197**, 20 (2011).
[74] B.-J. Cai and L.-W. Chen, Phys. Rev. C **85**, 024302 (2012).
[75] N. Kaiser, Phys. Rev. C **91**, 065201 (2015).
[76] M. Oertel, M. Hempel, T. Klähn, and S. Typel, Rev. Mod. Phys. **89**, 015007 (2017).
[77] C. Wellenhofer, J. W. Holt, and N. Kaiser, Phys. Rev. C **93**, 055802 (2016).
[78] R. Wang and L.-W. Chen, Phys. Lett. B **773**, 62 (2017).
[79] H. Jiang, M. Bao, L.-W. Chen, Y. M. Zhao, and A. Arima, Phys. Rev. C **90**, 064303 (2014).
[80] J. Xu, L.-W. Chen, B.-A. Li, and H.-R. Ma, Phys. Rev. C **75**, 014607 (2007).
[81] B. K. Agrawal, J. N. De, S. K. Samaddar, M. Centelles, and X. Viñas, Eur. Phys. J. A **50**, 19 (2014).